# On the functional lifetime of near field metallic plasmonic transducers in heat assisted magnetic recording (HAMR)

*Bair V. Budaev and David B. Bogy*
*University of California*
*Etcheverry Hall, MC 1740,*
Berkeley, CA 94720-1740, U.S.A.

*E-mails: bair@berkeley.edu, dbogy@berkeley.edu*

February 16, 2012

## Abstract

For a HAMR system to be successful it must deliver heat to a small spot on a magnetic disk without being damaged by the applied power. This paper shows that such conditions may not be easily attained in systems that use laser energy and plasmonic near field transducers. It is also shown that the analysis and design of the near field transducers cannot rely on the often used numerical integration of the conventional Maxwell equations of electrodynamics of continuous media, because such equations implicitly incorporate numerous assumptions that are not valid in nanoscale systems. Here we examine all assumptions inherent in the derivation of these equations and point out which assumptions are violated if they are applied to the metallic nanoscale elements of HAMR systems. The main body of the paper focusses on the well-known experimental results that support our conclusions while the derivations are relegated to the appendices.

## 1 Introduction

The idea of creating focused light rays *"powerfull enough to cut through a railway bridge in a few seconds. ...pierce, and cut through and destroy everything",* [31, Sec.43], had been circulating long before the high power sources of laser light became available. Not surprisingly, as soon as lasers were invented they found numerous applications in various fields going far beyond straightforward material processing and weaponry. In particular, lasers reshaped the digital data storage technology, making optically recorded DVDs and CDs the dominant carriers in household video and audio collections. More recently, attempts have been made to use optical energy in thermally assisted magnetic recording hard disk drives (TAR or HAMR), where the focused light is employed to heat a small spot of magnetic material on a disk to a level sufficient to lower its resistance to magnetization by the limited flux level of the closely spaced writing head. If successful such systems promise significant increase of data storage density, but to be successful, they must either overcome the technical difficulty of focusing light onto a spot ($\sim 25$nm) considerably smaller than its wavelength ($\sim 500$nm), or use radiation with shorter wavelength, or employ an alternative, non-optical, method

of local heating.

Most HAMR systems currently under development rely on plasmonic devices which receive light generated by a laser, convert it to plasmonic waves propagating along the surface of a near field transducer element towards the tip that is located within a few nanometers from the recording medium [7, 9, 17, 28, 29]. Plasmonic waves at the tip of the transducer are coupled with electromagnetic fields and currents in the recording layer to heat a spot in the medium located across the few nanometers gap from the tip. The feasibility of such a method of local heating is confirmed by several plasmonic-based prototypes of HAMR systems which were able to write data tracks of sufficiently small size and good quality, [7, 9, 17, 20, 28, 29]. However, these prototypes reportedly survive only a few writing cycles, and since there are no clear reasons explaining such a short life time [8, 9] the prospects of the plasmonic-based design of HAMR systems remain unclear.

One of the plausible explanations for the fast deterioration of HAMR prototype systems is that their near field transducers absorb a substantial part of the energy that is supposed to be transmitted to the recording medium and are heated by this energy to temperatures above the threshold that causes their structural damage or even partial melting. This hypothesis is supported by the published data [7, 17, 20] that consistently imply that part of the surfaces of the near field transducers receive optical radiation with a density of the order $\sim 10\text{MW/cm}^2$, which is known to be high enough to cause overheating and structural damage of many metals, and especially of thin metallic films, [1, 2, 10, 18, 19, 21–23, 25, 27, 30, 33]. However, such explanation cannot be easily verified because, on one hand, there are no measurements of the temperature in the near field transducers, but on the other hand, some numerical simulations have shown that the transducers remain practically unheated even while they heat the recording spots to about 400℃. Such simulations are based on multi-physics models that are supposed to take into account all of the involved optical-electromagnetic-thermal phenomena, but the reliability of such simulations appears to be questionable because they are based on macroscopic Maxwell equations and constitutive material relations, which may not be valid for the analysis of nanoscale objects because they are generally not valid in a few nanometers thick surface layer comparable with the mean path traveled by conduction electrons in one cycle of oscillations. All of the above motivated this current study that is intended to clarify the limits of applicability of the standard methods of analysis of the phenomena in nanoscale near field transducers, and to understand the reasons for the lower than expected durability of existing prototypes of HAMR systems.

The limitations of the macroscopic theory of electrodynamics of continua in nano-scale systems is examined in this report by returning to the basic physics where assumptions were made in the derivation of these equations regarding the conditions for their validity. These assumptions are explicitly formulated in many textbooks [11, 15], but have largely been ignored in numerical simulation codes that provide generally reliable solutions of the Maxwell equation in macro scale systems, where most of these assumptions appear to not be formally violated. However, applications
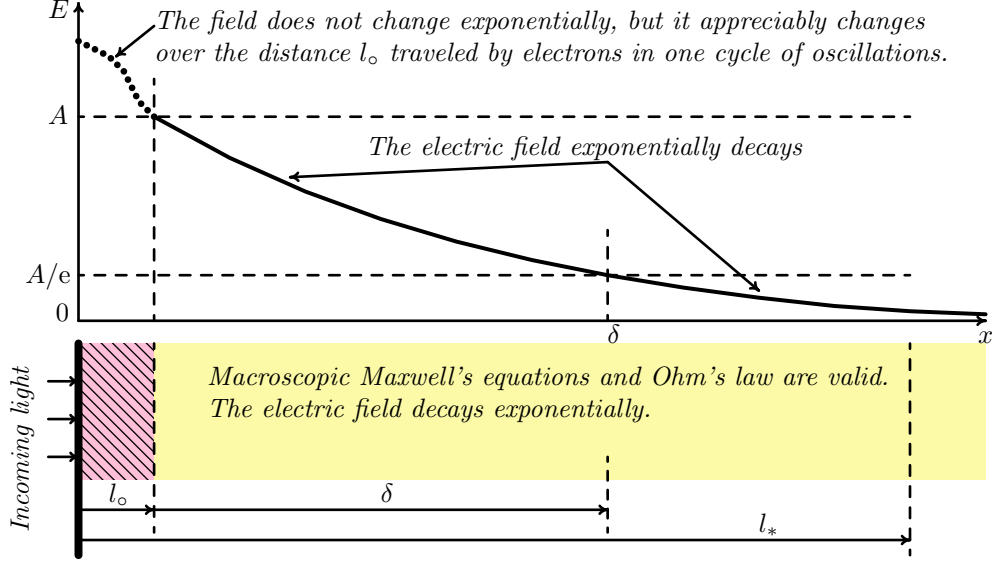
of these codes to nanoscale systems inherent in HAMR applications may become meaningless in cases when the underlying assumptions do not hold. We examine the derivation of the Maxwell equations and corresponding constitutive material relations, especially in metals, and identify the instances, relevant to HAMR, when the conventional equations may not be valid. We relegate this development to the appendices at the end of this article so as to avoid distracting readers from our main results and message.

## 2  Damage of metal surfaces caused by laser irradiation

Since light is a form of electromagnetic radiation its interaction with metals is customarily described in terms of the macroscopic Maxwell equations, which, as discussed in the appendices, are well justified but not complete, as they need to be accompanied by constitutive relations connecting the electric and magnetic fields $\boldsymbol{E}$ and $\boldsymbol{B}$ with the polarization $\boldsymbol{P}$, magnetization $\boldsymbol{M}$ and current $\boldsymbol{J}$. If these relations can be reduced to direct proportionalities $\boldsymbol{J} = \sigma\boldsymbol{E}$, $\boldsymbol{P} = \chi\boldsymbol{E}$ and $\boldsymbol{M} = \chi_m\boldsymbol{B}$, with spatially homogeneous coefficients, then the interaction of light with the metal can be described by a rather simple and well developed method. Thus, monochromatic fields induced in the metal can be represented as linear combinations of plane waves with complex-valued wave vectors. In particular, the current near the metal's surface is described by $\boldsymbol{J} = \boldsymbol{J}_0\mathrm{e}^{-px}$, where $x$ is the distance from the surface, $p$ is a frequency-dependent material parameter with $\mathrm{Re}(p) > 0$, and $\boldsymbol{J}_0$ is the current on the surface. Since the induced current is localized in the skin layer near the surface, the corresponding Joule heat $Q = \boldsymbol{J}^2/\sigma$ is generated only inside the skin layer, but once produced the heat diffuses into the metal by the conduction mechanisms described by the classical heat equation. As the metal heats, its material parameters change and the macroscopic Maxwell equations, constitutive relations, Ohm's law and the heat equation form a complicated system of non-linear equations which can only be studied by numerical methods.

The outlined description of the interactions between light and metals is not simple, but it is rather transparent and can be studied by well-developed numerical methods, including those implemented in commercial software packages. However, this model does not take into account the existence of a very thin surface layer $S_h$ of a few nanometers thickness comparable with the mean free path traveled by conduction electrons in one cycle of the light oscillations, as explained in Appendices 2, 4. In this layer, show in Fig. 1 the current $\boldsymbol{J}$ and polarization $\boldsymbol{P}$ are not proportional to the electric field $\boldsymbol{E}$, but depend on the values of $\boldsymbol{E}(\xi)$ within the entire layer [13, 16]. As a result, the amount of heat generated in the layer $S_h$ cannot be described by the Joule formula $Q = \boldsymbol{J}^2/\sigma$, and, consequently, this formula can no longer be an input term for the heat conduction equation describing heat flow in the metal.

Since the width of the surface layer $S_h$ does not exceed a few nanometers, its influence on the metal's reaction to light in most cases is negligible. However, there are situations when this layer plays an important role and cannot be neglected. Obviously, this layer cannot be ignored in the

*The field does not change exponentially, but it appreciably changes over the distance $l_\circ$ traveled by electrons in one cycle of oscillations.*

*The electric field exponentially decays*

*Macroscopic Maxwell's equations and Ohm's law are valid. The electric field decays exponentially.*

$l_\circ$ *is the mean free path of conduction electrons in one cycle of oscillations ($l_\circ = 2\pi v_F/\omega \sim 3$nm),*
$\delta$ *is the distance over which the field exponentially decays by $e$ times ($\delta \approx c/\omega_p \sim 20$nm),*
$l_*$ *is the mean free path of conduction electrons between collisions ($l_* = v_F/\gamma \sim 30$nm),*
*where: $v_F$ – speed of electrons, $\gamma$ – frequency between collisions, $\omega_p$ – plasma frequency*
*(See Appendix 4 for detail)*

Figure 1: Penetration of light into a metal

analysis of light interaction with metal films thinner than $20 - 30$ nanometers. It is also clear that this layer should be taken into account whenever surface phenomena are important, as, for example, in cases when the film's surface is intended to relay power to another receptor. Another important scenario where the surface layer $S_h$ cannot be ignored is related with the survival of metals under prolonged irradiation by sufficiently powerful light. Indeed, since the absorbtion of electromagnetic radiation by metals starts at the surface and then diffuses into the interior, the temperature near the surface may be considerably higher than deeper inside. In particular, immediately after the radiation is turned on the surface temperature may briefly rise to the level sufficient for local structural damage or even partial melting. Then, as the heat is conducted into the interior of the metal the surface may cool, but structural damage may accumulate and lead to eventual destruction of the surface in an undesirably short period of time.

The failure of the local Ohm's law makes the laser heating of metal surfaces difficult for modeling because the models can no longer be reduced to differential equations, but the introduction of more complex models, based on integro-differential equations, for example, may not make the theoretical prediction more reliable or accurate. It is well known [22] that the additional heating of metal surfaces is caused by additional "surface" scattering of conduction electrons that can be described in terms of the frequency of surface collisions. However, this additional frequency is highly sensitive to the surface roughness, purity and even to the presence of surface waves, which may be excited

4

by the same laser radiation that causes heating. As a result, the additional surface heating is included into the theory with a fitting factor $0 < p < 1$, which may change the output by an order of magnitude [22], and thus it reduces the value of numerical simulations for the design of precision devices which use lasers for the heating of metals.

The above implies that the design of laser-based HAMR systems cannot rely on numerical simulations to provide better than order-of-magnitude estimates and should take into account the vast experimental evidence of metal damage caused by laser radiation of intensity comparable to or even weaker than that used in HAMR systems currently under development.

It is well known that the severity of the laser induced damage of metal depends on the frequency of radiation, pulse duration and its shape, repetition rate, the current temperature of the metal [1, 19, 22, 23, 25], and even the presence of plasmonic waves, which may significantly enhance heating [32] and cause the surface deterioration by formation of surface periodic structures [3, 4, 6, 22]. Thus, the heating rate of metals generally increases as the frequency of the radiation moves from the infrared towards the ultraviolet range of the spectrum [22]. One of the reasons for such increase is the increase of absorptivity which may be very noticeable. Thus, the absorptivity of Au used in most HAMR prototypes, increases from $\sim 5\%$ at $\lambda \approx 700$nm to above $\sim 50\%$ at $\lambda \approx 500$nm. The absorptivity of metals can also increase by up to a factor of four when the temperature increases from room temperature to the melting point[5, 21]. Such behavior of the absorptivity creates a positive feedback which may trigger accelerated heating after a certain level is achieved.

Apart from the total incidence power, the duration of the laser pulse appears to be the most important parameter determining the laser induced damage of metals. Since conduction electrons reach thermal equilibrium with the lattice in the time scale of $10^{-11}$s, the mechanisms of laser interaction with metals are different for irradiation by ultrashort pulses, shorter that $10^{-12}$s, by pulses with duration in the nano/microsecond range, by pulses longer than a millisecond, which are not much different than continuous radiation, and by pulses from a crossover millisecond range, which have features of the both pulsed and continuous radiation.

For lasers with millisecond or longer pulses, the damage threshold is determined by the areal density of power $(\mathrm{W/cm}^2)$ and is generally independent on the duration of the radiation. But the damage threshold caused by a pulsed laser heavily depends on the pulse duration, and if the threshold is measured in terms of power density $(\mathrm{W/cm}^2)$ then it is inversely proportional to the square root of the pulse duration. However, the damage threshold of pulsed lasers is usually characterized in terms of the fluence $(\mathrm{J/cm}^2)$ and, thus, in this unit it is proportional to the square root of the pulse duration. The use of different characterizations of the damage thresholds makes it difficult to compare the effects of continuous and pulsed radiations, but there is a rather simple "rule of thumb" implying that the damage threshold of a continuous laser measured in $\mathrm{W/cm}^2$ is usually a factor of $10^4$–$10^5$ higher than the value of the threshold of a microsecond pulse measured in $\mathrm{J/cm}^2$, [26]. It is easy to see that this rule agrees with the above mentioned relationship between

the damage threshold and the duration of the irradiation. Indeed, this rule implies that if $x\,\mathrm{J/cm^2}$ is a damage threshold of a microsecond pulse, then a millisecond pulse has a threshold of about $\sqrt{1000}\,x\,\mathrm{J/cm} \sim 30x\,\mathrm{J/cm}$, which is equivalent to $3 \cdot 10^4 x\,\mathrm{W/cm}$ in the units used for continuous irradiations, which is similar to the irradiation by pulses longer than a millisecond. Although the scaling of laser induced damage thresholds may not be exact, it provides a reasonable opportunity to compare the vast amount of experimental data accumulated over almost fifty years of studies and collected in an extensive literature, including the reports from the annual Conference on laser-induced damage of optical materials held in Boulder, Colorado, since 1969, [30].

Since the prototypes of HAMR systems get their optical energy from lasers with wavelength $\sim 800$nm and convert it to heat using near field transducers made from Au, we now limit ourselves to a review of the experimental data for the damage of gold and gold films by laser radiation in the visible part of the spectrum.

In [18, 21] the thresholds of the damage for Au, Ag, Cu are studied for lasers operating at 492nm, 1060nm and longer wavelengths. The experiments with a 492nm laser are made using 500ns pulses, and the experiments with 1060nm laser are made with 9ns pulses. Nevertheless, despite the rather different conditions, when the results of these reports are re-scaled to a continuous mode of operation, they both predict comparable damage thresholds $\sim 10^6 \mathrm{W/cm^2}$, for slip damage (irreversible mechanical damage), and $\sim 10^7 \mathrm{W/cm^2}$ for damage from melting. Although these studies don't specify the nature of the mechanical "slip" damage, the threshold of such damage agrees with the results from [10], which report structural transformations of metals (Al, Cu, Cr, Ni, Ti) exposed to laser radiation. In particular, it is shown in [10] that when laser pulses ranging from 80ns to several milliseconds at the wavelengths $\lambda = 1060$nm and $\lambda = 694$nm, reach the power density $\sim 10^5 \mathrm{W/cm^2}$ then the irradiated metals undergo such structural transformation as recrystallization and the formation of pores. Although the goals of the studies [10, 18, 21, 33] appear to be unrelated, their results are well correlated and suggest that the deterioration of thin metal films may be caused by laser irradiation with the power density $10^5 \mathrm{W/cm^2}$, which is below the level reported in the prototypes of HAMR systems.

## 3    Conclusion

The above notes suggest that energy delivery paths in laser-based HAMR systems may be self-destructive because they need to sustain laser irradiation of the level comparable to or even exceeding laser induced damage thresholds for the materials used in such devices. Moreover, the excitation of plasmonic oscillations intended to improve the efficiency of near field transducers may also accelerate the destruction of the transducers. Therefore, it appears that to design a successful HAMR system employing laser-energized plasmonic transducers it is necessary to admit that these transducers are exposed to rather powerful irradiation which may cause heating and structural damage. Correspondingly, the design of such systems should take special care to both protect the

near field transducers and thermally insulate them from the rest of the magnetic head.

## References

[1] S. I. Anisimov, Ya. A. Imas, G. S. Romanov, and Yu. V. Khodyko, *Action of powerful radiation on metals*, Nauka, Moscow, 1970. (in Russian).

[2] Fedorov V. B. (ed.), *Effects of laser radiation on absorbing condensed matter*, Proceedings of the Institute of General Physics, Nova Science Publishers, Academy of Sciences of the USSR, Commack, New York, 1990.

[3] T. J. Bastow, *Ordetring of microcraters produced by a laser on a metal surface*, Nature **222** (1969), no. 5198, 1058–1060.

[4] V. V. Bazhenov, A. M. Bonch-Bruevich, R. I. Petrushkyavichyus, Yu. I. Rexnis, M. N. Libenson, V. S. Makin, and V. V. Trubaev, *The role of SEW in the effect of CW scanned laser radiation on metals*, Technical Physics Letters **12** (1986), no. 3, 151–156.

[5] A. M. Bonch-Bruevich and Ya. A. Imas, *title*, Soviet Physics - Technical Physics **12** (1968), 1407.

[6] A. M. Bonch-Bruevich, M. N. Libenson, V. S. Makin, and V. V. Trubaev, *Surface electromagnetic waves in optics*, Optical Engineering **31** (1992), no. 4, 718–730.

[7] M. Chabalko, E. Black, S. Powell, Y. Kong, Y. Luo, T. E. Schlesinger, and J. Bain, *Evanescently coupled near field transducers for HAMR*, Digest of the 22nd magnetic recording conference TMRC-2011, 2011August, pp. 69–70.

[8] W. A. Challener, E. C. Gage, and C. Peng, *Optical transducers for near field recording*, Japanese Journal of Applied Physics **45** (2006), no. 8B, 6632–6642.

[9] W. A. Challener, C. Peng, A. V. Itagi, D. Karns, W. Peng, Y. Peng, X. Yang, X. Zhu, Y.-T. Gokekemeijer N. J. Hsia, G. Ju, R. E. Rottmayer, M. A. Seigler, and E. C. Gage, *Heat-assisted magnetic recording by a near-field transducer with efficient optical energy transfer*, Nature photonics **3** (2009), 220–224.

[10] A. M. Chaplanov and E. I. Tochinsky, *Laser-induced structural tranformations in thin metal films*, Thin solid films **116** (1984), 117–128.

[11] R. P. Feynman, R. B. Leighton, and M. L. Sands, *The Feynman lectures on physics, v. 1*, 3rd ed., Pearson/Addison-Wesley, 2006.

[12] P. W. Gilberd, *The anomalous skin effect and the optical properties of metals*, Journal of Physics F: Metal Physics **12** (1982), no. 8, 1845–1860.

[13] R. N. Gurzhi, M. Ya. Azbel, and X. B. Lin, *Surface effects in infrared optics*, Solid state physics **5** (1963), no. 3, 759–768.

[14] C. Kittel, *Introduction to solid state physics*, John Willey & Sons, 1976.

[15] L. D. Landau and E. M. Lifshitz, *Electrodynamics of continuous media*, Course of Theoretical Physics, v. 8, Pergamon Press, 1960.

[16] I. M. Lifshits, M. Ya. Azbel', and M. I. Kaganov, *Electron theory of metals*, Consultants Bureau, Adam Hilger, New York, London, 1973.

[17] D.-S. Lim, M-H. Shin, H.-S. Oh, and Y.-J. Kim, *Opto-thermal analysis of novel heat assited magnetic recording media based on surface plasmon enhancement*, IEEE Transaction on Magnetics **45** (2009), no. 10, 3844–3847.

[18] C. D. Marrs, W. N. Faith, J. N. Dancy, and J. O. Porteus, *Pulsed laser-induced damage of metals at 492 nm*, Applied Optics **21** (1982), no. 22, 4063–4066.

[19] G. P. Mueller, *The effects of CW and RP lasers on composites and metals*, Technical Report NRL/MR/665–95-7773, Naval Research Laboratory, Washington, D. C., 1995.

[20] C. Peng, W. A. Challener, A. Itagi, and E. C. Gage, *Surface-plasmon resonance of a planar near-field optical transducer*, Digest of the 22nd magnetic recording conference TMRC-2011, 2011August, pp. 71–72.

[21] J. O. Porteus, D. L. Decker, W. N. Faith, D. J. Grandjean, S. C. Seitel, and M. J. Soileau, *Pulsed laser-induced melting of precision diamond-machined cu, ag, and au at infrared wavelength*, IEEE Transactions of Quantum Electronics **17** (1981), no. 10, 2078–2085.

[22] A. M. Prokhorov, V. I. Konov, I. Ursu, and I. N. Mihăilescu, *Laser heating of metals*, The Adam Hilger Series on Optics and Optoelectronics, Adam Hilger, Bristol, Philadelphia, New York, 1990.

[23] J. F. Ready, *Effects of high-power laser radiation*, Academic Press, New York, London, 1971.

[24] G. E. H. Reuter and E. H. Sondheimer, *The theory of the anomalous skin effect in metals*, Proceedings of the Royal Society of London. A. **195** (1948), 336–364.

[25] J. T. Schriempf, *Response of materials o laser radiation: a short course*, NRL Report 7728, Naval Research Laboratory, Naval Research Laboratory, D.C., 1974.

[26] *Laser damage threshold*, Semrock, Inc, Rochester, NY 14624, 2011. http://www.semrock.com/laser-damage-threshold.aspx.

[27] M. J. Soileau, *Laser-induced damage to optical materials*, Handbook in optics, McGraw-Hill, New York, 2010.

[28] B. C. Stipe, T. C. Strand, Ch. C. Poon, H. Balamane, J. A. Katine, J.-L. Li, V. Rawat, H. Nemoto, A. Hirotsune, O. Hellwig, R. Ruiz, E. Dobisz, D. S. Kercher, N. Robertson, T. R. Albrecht, and B. Terris, *Magnetic recording at* $1.5\text{pbm}^{-2}$ *using an integrated plasmonic antenna*, Nature photonics **4** (2010), 484–488.

[29] K. Takano, E. Jin, T. Maletsky, E. Schreck, and M. Dovek, *Optical design challenges of thermally assisted magnetic recording heads*, IEEE Transaction on Magnetics **46** (2010), no. 3, 1130–1138.

[30] *Proceedings of laser-induced damage to optical materials*, SPIE, the Inernational Society of for Optical Engineering, Bellingham, WA, annual. (since 1969).

[31] A. Tolstoy, *The Garin death ray*, University Press of the Pacific, Honolulu, Hawaii, 2001. (1st Russian edition published in 1927. English editions: 1st in 1936 revised in 1955).

[32] T. Tsang and D. D. Smith, *Surface-enhanced nonequilibrium electronic heating in thin films due to the excitation of single metal-boundary surface plasmons*, Optics communications **70** (1989), no. 2, 115–118.

[33] T. Turner, *High laser-induced-damage threshold optics. what you need to know about laser damage before you buy laser optics and what questions you need to ask your vendor*, Electronic publication: Photonics.com (2011, March). http://photonics.com/article.aspx?AID=46171.

[34] A. H. Wilson, *The theory of metals*, Cambridge University Press, London, 1965.

[35] F. Wooten, *Optical properties of solids*, Academic Press, New York, London, 1972.

[36] J. M. Ziman, *Electrons and phonons*, Oxford University Press, 1962.

## Appendix 1: Optical fields in a medium

It is well known that most electromagnetic phenomena can be described by the Maxwell equations

$$\boldsymbol{\nabla} \cdot \boldsymbol{B}_* = 0, \qquad\qquad \boldsymbol{\nabla} \times \boldsymbol{E}_* + \frac{\partial \boldsymbol{B}_*}{\partial t} = 0, \qquad\qquad (A1.1)$$

$$\boldsymbol{\nabla} \cdot \boldsymbol{E}_* = \frac{\rho_*}{\epsilon_0}, \qquad\qquad c^2 \boldsymbol{\nabla} \times \boldsymbol{B}_* - \frac{\partial \boldsymbol{E}_*}{\partial t} = \frac{\boldsymbol{J}_*}{\epsilon_0}, \qquad\qquad (A1.2)$$

where $\epsilon_0$ is the permittivity of vacuum and $c$ is the speed of light in vacuum, $\boldsymbol{E}_*$ and $\boldsymbol{B}_*$ are the electric and magnetic fields, $\rho_*$ is the density of electric charges, and $\boldsymbol{J}_* = \rho_* \boldsymbol{v}_*$ is the current introduced in terms of the charge density and the charge's velocity $\boldsymbol{v}_*$.

Although these equations are usually referred to as Maxwell's equations in free space (vacuum), they actually describe electromagnetic phenomena everywhere, including inside a medium, but to use them in a medium it is necessary to track all elementary charges in the medium. Since it is not feasible to take into account every electron and proton, even in micro or nano-sized material bodies, the electromagnetic phenomena in a medium are usually described by the macroscopic Maxwell equations obtained by averaging the equations (A1.1), (A1.2) over domains that contain a large number of charged particles but are small compared to the distance over which the involved fields change appreciably.

Let every point $x$ inside a material body be surrounded by a small domain $G_x$ that contains a statistically significant number of elementary charges but, at the same time, is small compared to all characteristic dimensions, including but not limited to the geometry of the body, wavelengths of

propagating waves, depths of penetration of evanescent waves, etc. Then, averaging the microscopic Maxwell equations (A1.1)–(A1.2) reduces them to the equations

$$\mu_0 \boldsymbol{\nabla} \cdot \boldsymbol{B} = 0, \qquad\qquad \boldsymbol{\nabla} \times \boldsymbol{E} = -\mu_0 \frac{\partial \boldsymbol{B}}{\partial t}, \qquad\qquad (\text{A1.3})$$

$$\epsilon_0 \boldsymbol{\nabla} \cdot \boldsymbol{E} = \rho_{\text{eff}}, \qquad\qquad \boldsymbol{\nabla} \times \boldsymbol{B} = \ \ \epsilon_0 \frac{\partial \boldsymbol{E}}{\partial t} + \boldsymbol{J}_{\text{eff}}, \qquad\qquad (\text{A1.4})$$

where $\boldsymbol{E}(x)$ and $\boldsymbol{B}(x)$ are the mean values of the microscopic electric and magnetic fields over the domains $G_x$, while $\rho_{\text{eff}}(x)$ and $\boldsymbol{J}_{\text{eff}}(x)$ are the mean values of the microscopic charges and currents over the same domains $G_x$.

It is important to recall that the effective charge density may not vanish even in an electrically neutral medium. To see this we first assume that when a neutral medium is not exposed to electromagnetic fields then its positive and negative charges are distributed homogeneously so that the effective charge density and current vanish, as if the medium does not contain any charges and currents. Although this assumption contradicts the atomistic theory, it provides a rather accurate approximation for the cases when $\rho(x)$ can be defined as the ratio $Q(G_x)/V(G_x)$, where $Q(G_x)$ and $V(G_x)$ are the total charge and volume of a small but still finite vicinity $G_x$ of the point $x$ containing a large number of charged particles. The situation changes when an electrically neutral medium is exposed to an electromagnetic field and its elementary charges move in different directions with different speeds causing inhomogeneities of the charge distribution and generating net currents.

The above suggests the decomposition of the effective density and current into two terms

$$\rho_{\text{eff}} = \rho + \rho_{\text{ind}}, \qquad \boldsymbol{J}_{\text{eff}} = \boldsymbol{J} + \boldsymbol{J}_{\text{ind}}, \qquad\qquad (\text{A1.5})$$

where the first terms $\rho$ and $\boldsymbol{J}$ represent the "external" charges and currents, while the second terms $\rho_{\text{ind}}$ and $\boldsymbol{J}_{\text{ind}}$ represent the charges and currents redistributed in the material due to the presence of the fields $\boldsymbol{E}$ and $\boldsymbol{B}$. This definition assumes that the integral of the charge density $\rho_{\text{ind}}$ over the entire body vanishes, which implies that it admits the representation

$$\rho_{\text{ind}} = -\boldsymbol{\nabla} \cdot \boldsymbol{P}, \qquad\qquad (\text{A1.6})$$

where $\boldsymbol{P}$ is usually referred to as polarization. Then introducing a new field $\boldsymbol{D} = \epsilon_0 \boldsymbol{E} + \boldsymbol{P}$ we reduce the first equation from (A1.4) to $\boldsymbol{\nabla} \cdot \boldsymbol{D} = \rho$. Similarly, (A1.6) makes it possible to re-arrange the continuity equation $\partial \rho_{\text{ind}}/\partial t + \boldsymbol{\nabla} \cdot \boldsymbol{J}_{\text{ind}} = 0$ to the form

$$\boldsymbol{\nabla} \cdot \left( -\frac{\partial \boldsymbol{P}}{\partial t} + \boldsymbol{J}_{\text{ind}} \right) = 0, \qquad\qquad (\text{A1.7})$$

which implies the existence of a vector field $\boldsymbol{M}$ such that

$$\boldsymbol{J}_{\text{ind}} - \frac{\partial \boldsymbol{P}}{\partial t} = \boldsymbol{\nabla} \times \boldsymbol{M}. \qquad\qquad (\text{A1.8})$$

Then, the second equation from (A1.4) can be re-written as $\boldsymbol{\nabla} \times \boldsymbol{H} = \partial \boldsymbol{D}/\partial t + \boldsymbol{J}$, where $\boldsymbol{H} = \epsilon_0 c^2 \boldsymbol{B} - \boldsymbol{M}$ is a new field usually called magnetic induction.

9

Summing up we get a system of macroscopic Maxwell equations

$$\boldsymbol{\nabla} \cdot \boldsymbol{B} = 0, \qquad \boldsymbol{\nabla} \times \boldsymbol{E} = -\frac{\partial \boldsymbol{B}}{\partial t}, \qquad (A1.9)$$

$$\boldsymbol{\nabla} \cdot \boldsymbol{D} = \rho, \qquad \boldsymbol{\nabla} \times \boldsymbol{H} = \frac{\partial \boldsymbol{D}}{\partial t} + \boldsymbol{J}, \qquad (A1.10)$$

where the pair of homogeneous equations (A1.9) involves only the electric and the magnetic fields $\boldsymbol{E}$ and $\boldsymbol{B}$, while the pair of inhomogeneous equations (A1.10) connects the charge density $\rho$ and the current $\boldsymbol{J}$ with the fields $\boldsymbol{D}$ and $\boldsymbol{H}$ defined by the expressions

$$\boldsymbol{D} = \epsilon_0 \boldsymbol{E} + \boldsymbol{P}, \qquad \boldsymbol{H} = \epsilon_0 c^2 \boldsymbol{B} - \boldsymbol{M}, \qquad (A1.11)$$

where $\boldsymbol{P}$ and $\boldsymbol{M}$ are the polarization and magnetization induced by the primary fields $\boldsymbol{E}$ and $\boldsymbol{B}$.

Finally, it is necessary to estimate the limitations of the macroscopic Maxwell equations introduced only as approximations. Since the macroscopic fields $\rho(x)$, $\boldsymbol{E}(x)$ and $\boldsymbol{B}(x)$ were introduced as averages over small domains $V_x$ they can only have meaning in domains that are considerably larger than the average "pixel" $V_x$. To estimate the size of $V_x$ we assume that the number density of atoms in a condensed matter is of the order of 100 atoms per cubic nanometer (it is about 50 for Au), and that the average atom has about 100 protons and electrons (158 for Au). Then, the average number of charges per cubic nanometer is of the order of $10^4$, and this estimate suggests that the atomic structure of matter limits the applicability of the macroscopic Maxwell equations to domains with linear dimensions larger than about one fourth of a nanometer. However, these equations also involve the current $\boldsymbol{J}$, polarization $\boldsymbol{P}$ and magnetization $\boldsymbol{M}$, which are introduced indirectly by a more sophisticated procedure than simple averaging of some microscopic fields. Correspondingly, these fields may apply additional limitations on the use of the macroscopic Maxwell equations, and in metals such limitations may become important in the nano-scale.

## Appendix 2: Ohm's law in metals

The Maxwell equations considered alone are not sufficient for the analysis of electromagnetic phenomena. Thus, the current $\boldsymbol{J}(\boldsymbol{x}, t)$ at a particular point $\boldsymbol{x}$ at a particular time $t$ depends on the velocities of elementary charges that are determined by the electromagnetic fields both at the present and at preceding times, by the mechanical properties of the charged particles, and by the obstacles to the particle's further motion caused by the surrounding medium. Therefore, in order to use the Maxwell equations it is first necessary to specify the relationship between the current $\boldsymbol{J}$ and the electromagnetic fields. Moreover, this relationship should be described in macroscopic terms, because a microscopic description is no more useful than the microscopic Maxwell equations.

In metals some electrons are bonded to atoms but there are also conduction electrons moving in the space between positively charged ions much like molecules in a regular Fermi gas. The mobility of the conduction electrons determines such characteristic properties of metals as their high thermal

and electric conductivity and the inability of the electric fields to penetrate deep under the metal's surfaces, which sharply distinguishes metals from dielectrics.

The similarity with a gas makes the kinetic theory a natural choice for the analysis of the properties of metals in terms of the distribution of the conduction electrons [16, 24, 34]. However, some characteristic properties of metals can be described in terms of the simplest free electron model in which each conduction electron appears as an independent particle moving inside the material and occasionally colliding with other objects in such a way that its states before and after each collision are uncorrelated. In this model the motion of an electron in an electromagnetic field is described by the Newtonian equation

$$m_*\ddot{\boldsymbol{x}} = q\big[\boldsymbol{E}(\boldsymbol{x},t) + \dot{\boldsymbol{x}} \times \boldsymbol{H}(\boldsymbol{x},t)\big], \tag{A2.12}$$

where $\boldsymbol{x}$ is the position of an electron, $q$ is the electron's charge, and $m_*$ is the electron's effective mass. This equation controls the motion of an electron only between collisions which follow each other at random times distributed by the Poisson law with a parameter $\gamma$, so that

$$P(t, t + \mathrm{d}t) = \gamma \mathrm{e}^{-\gamma t}\mathrm{d}t, \tag{A2.13}$$

is the probability of the next collision happening within the time interval $(t, t + \mathrm{d}t)$ after the preceding collision. It is well known that $\gamma$ coincides with the average number of collisions per unit time and $\tau = 1/\gamma$ coincides with the average time between consecutive collision [15, 35]. For this reason, $\gamma$ is often referred to as the frequency of collisions, and $\tau$ as a mean time between collisions.

Although the right-hand part of (A2.12) contains both the electric and magnetic fields, it is well known that the term representing the latter can be ignored [15]. Then, assuming that $\boldsymbol{E}(x)$ is known we integrate the differential equation (A2.12) and find that in the time interval $(t_n, t_{n+1})$ between two consecutive collisions, the path of the electron satisfies the conditions

$$\dot{\boldsymbol{x}}(t) = \boldsymbol{v}_n + \frac{q}{m_*}\int_{t_n}^t \boldsymbol{E}(\boldsymbol{x}(s), s)\mathrm{d}s, \qquad\qquad t_n < t < t_{n+1}, \tag{A2.14}$$

$$\boldsymbol{x}(t) = \boldsymbol{x}_n + (t - t_n)\boldsymbol{v}_n + \boldsymbol{\xi}(t), \qquad\qquad t_n < t < t_{n+1}, \tag{A2.15}$$

where $\boldsymbol{x}_n$ and $\boldsymbol{v}_n$ are the initial conditions of the motion on the considered time interval, and $\boldsymbol{\xi}(t)$ is a non-trivial motion defined by the conditions

$$\boldsymbol{\xi}(t) = \frac{q}{m_*}\int_{t_n}^t (t - s)\boldsymbol{E}(\boldsymbol{x}_n + (s - t_n)\boldsymbol{v}_n + \boldsymbol{\xi}(s), s)\mathrm{d}s, \qquad t_n < t < t_{n+1}, \tag{A2.16}$$

which can be treated as an integral equation with two yet indefinite parameters $\boldsymbol{x}_n$ and $\boldsymbol{v}_n$.

To specify $\boldsymbol{x}_n$ and $\boldsymbol{v}_n$ we recall that the equations (A2.12) and (A2.15)–(A2.16) control the motion of the electron only between collisions. Therefore the position $\boldsymbol{x}_n$ of the electron immediately after the $n$-th collision is completely determined by the electron's past. On the other hand, the

velocity of the electron $\boldsymbol{v}_n$ immediately after the $n$-th collisions is considered as random. In the simplest model, it is represented as $\boldsymbol{v}_n = v_F \boldsymbol{e}_n$, where $\boldsymbol{e}_n$ is a random uniformly distributed unit vector and $v_F$ is the Fermi speed, which is typically of the order of $v_F \sim 10^6 \text{m/s}$, [16, 22, 34, 35].

To verify that the outlined description of the electron's motion makes sense we use it to compute the electric conductivity in the case of the monochromatic electric field

$$\boldsymbol{E}(\boldsymbol{x}, t) = \boldsymbol{E} \mathrm{e}^{\mathrm{i}\omega t}, \tag{A2.17}$$

where $\boldsymbol{E}$ is a constant vector. In this case the expressions (A2.14) and (A2.15) reduce to

$$\dot{\boldsymbol{x}}(t) = v_F \boldsymbol{e}_n - \frac{\mathrm{i}q\boldsymbol{E}\mathrm{e}^{\mathrm{i}\omega t}}{m_* \omega} \left(1 - \mathrm{e}^{-\mathrm{i}\omega T}\right), \tag{A2.18}$$

$$\boldsymbol{x}(t) = \widetilde{\boldsymbol{x}}_n(t) - \frac{q\boldsymbol{E}\mathrm{e}^{\mathrm{i}\omega t}}{m_* \omega^2} \left(1 - \mathrm{e}^{-\mathrm{i}\omega T}\right), \tag{A2.19}$$

where

$$\widetilde{\boldsymbol{x}}_n(t) = \boldsymbol{x}_n + (t - t_n) \left[ v_F \boldsymbol{e}_n + \frac{\mathrm{i}q\boldsymbol{E}\mathrm{e}^{\mathrm{i}\omega t_n}}{m_* \omega} \right] \tag{A2.20}$$

is a uniform translation started at the time $t_n$ of the last collision, and $T = t - t_n$ is the time elapsed after that collision. Then the current $\boldsymbol{J}(\boldsymbol{x}, t)$ can be evaluated by the formula

$$\boldsymbol{J}(\boldsymbol{x}, t) = qN \langle \dot{\boldsymbol{x}}(t) \rangle, \tag{A2.21}$$

where $N$ is the number density of conduction electrons and the brackets $\langle \cdot \rangle$ denote the averaging over the random unit vector $\boldsymbol{e}_n$ and the random time $T$ between collisions.

Consider first the case when a metal occupies the entire space. In this case, to compute $\boldsymbol{J}(\boldsymbol{x}, t)$ it suffices to substitute (A2.18) into (A2.21) and observing that $\langle \boldsymbol{e}_n \rangle = 0$ reduce the averaging over the Poisson random number $T$ to the integral

$$\boldsymbol{J}(\boldsymbol{x}, t) = \gamma \int_0^\infty \dot{\boldsymbol{x}}(t) \mathrm{e}^{-\gamma T} \mathrm{d}T = \frac{q^2 N \boldsymbol{E} \mathrm{e}^{\mathrm{i}\omega t}}{\mathrm{i}\omega m_*} \left(1 - \gamma \int_0^\infty \mathrm{e}^{-(\gamma + \mathrm{i}\omega)T} \mathrm{d}T \right) \tag{A2.22}$$

which leads to the expression

$$\boldsymbol{J}(\boldsymbol{x}, t) = \frac{q^2 N \boldsymbol{E} \mathrm{e}^{\mathrm{i}\omega t}}{m_*(\gamma + \mathrm{i}\omega)} = \frac{q^2 N \boldsymbol{E}(\boldsymbol{x}, t)}{m_*(\gamma + \mathrm{i}\omega)}. \tag{A2.23}$$

As a result we get Ohm's law

$$\boldsymbol{J}(\boldsymbol{x}, t) = \sigma(\omega) \boldsymbol{E}(\boldsymbol{x}, t), \tag{A2.24}$$

with the complex-valued, frequency-dependent but $\boldsymbol{x}$-independent conductivity

$$\sigma(\omega) = \frac{\sigma_0 \gamma}{\gamma + \mathrm{i}\omega}, \tag{A2.25}$$

defined in term of the material constant

$$\sigma_0 = \frac{q^2 N_*}{m_* \gamma}, \tag{A2.26}$$

which is widely known as the DC-conductivity [14, 15, 35, 36].

It is easy to see that the derivation of (A2.25) relies on the assumption that the metal occupies the entire space. Indeed, this formula results from the integration in (A2.23) from $T = 0$ to $T = \infty$, where $T$ is the time elapsed after the last collision of the considered electron. Therefore, this computation takes into account electrons which arrive at $\boldsymbol{x}$ after infinitely long collision-free trajectories which are defined by (A2.19) as superpositions of a fast translational motion with the speed $v_F \sim 10^6$m/s along a random direction $\boldsymbol{e}_n$ and of small fluctuations with the amplitude proportional to $\boldsymbol{E}$ and inversely proportional to the frequency $\omega \sim 10^{15}$rad/s. All of these imply that the expression (A2.25) for $\sigma(\omega)$ takes into account electrons arriving at $\boldsymbol{x}$ after a long-distance flight along an almost straight path, which is unrealistic because such a path must originate at the point of the previous collision of the considered electron inside the body.

At first thought the above reasoning suggests that the conductivity of a finite piece of metal can never be computed by the formula (A2.25) because it takes into account contributions of the electrons moving along trajectories which do not fit inside any finite body. However, a closer analysis reveals that (A2.25) provides a rather accurate approximation of the conductivity of a metal anywhere except in a sufficiently thin boundary layer whose depth is determined by the frequencies $\gamma$ and $\omega$ of the collisions and field's oscillations.

To formulate the criteria of applicability of (A2.25) it suffices to notice that the integral in (A2.23) can be accurately approximated by the integral over a short interval $0 < T < T_{\gamma,\omega}$ with the upper limit just a few times larger than $(\gamma^2 + (\omega/2\pi)^2)^{-1/2}$. This implies that the current at the point $\boldsymbol{x}$ is essentially affected only by the electrons arriving at $\boldsymbol{x}$ after the collision within the distance $h \sim v_F T_{\gamma,\omega}$ from $\boldsymbol{x}$. Therefore, the expression (A2.25) for the conductivity of a metal is justified everywhere except for the boundary layer of thickness $h$, where

$$h \sim \begin{cases} l_* = v_F/\gamma, & \text{if} \quad \gamma \gg \omega/2\pi, \\ l_\circ = 2\pi v_F/\omega, & \text{if} \quad \gamma \ll \omega/2\pi, \end{cases} \tag{A2.27}$$

where $l_*$ is the mean free path of the conduction electron between consecutive collisions and $l_\circ$ is the mean free path traveled by a conduction electron in one cycle of the field oscillations.

Since in metals at room temperature the frequency of collisions and the speed of the electrons have the orders $\gamma \sim 10^{14}$s$^{-1}$ and $v_F \sim 10^6$m/s, respectively [16, 22, 35], the above analysis shows that in the infrared band $\omega < 10^{13}$rad/s the Ohm's law (A2.24), (A2.25) fails in the boundary layer comparable with the electrons's mean free path $l_* \sim 30$nm. However, in the optical band $\omega \sim 10^{15}$rad/s Ohm's law (A2.24), (A2.25) fails in the layer comparable with the ratio $l_\circ \sim 3$nm.

The failure of the Ohm's law in a thin boundary layer of a metal at room temperature has been known for a long time [16, §47], but for most applications a few nanometers wide layer is so thin that it can be ignored because it affects neither the penetration of light into the metal nor the reflection of light from the metal [12, 25, 35]. On the other hand, there are situations where even weak processes in a very thin boundary layer may not be ignored. For example, a few nanometers

wide layer cannot be ignored if the studied piece of metal is itself only about 20 nanometers thick. It is also clear that processes in a thin boundary layer may be important in cases of prolonged irradiation. Indeed, since the electrons in the boundary layer collide more frequently than inside the metal, the resistance in the boundary layer is higher than inside the body, and, therefore, the surface of the metal gets hotter than at locations deeper inside the body. As shown in numerous studies, the temperature near the surface of a metal may reach levels close to the melting point even when the metal inside remains relatively cool, and in the case of prolonged exposures, the surface layer may deteriorate, increasing its resistance and thus increasing the rate of further deterioration, [1, 22, 25].

To estimate the current in the boundary layer where Ohm's law (A2.24), (A2.25) fails it is necessary to take into account the asymmetry between the electrons arriving from the interior of the metal and the electrons arriving from the surface. Thus the contribution of the electrons arriving from the interior may be estimated by a formula like (A2.22) with the same frequency of collisions $\gamma$ which is typical deep in the metal. However, the electrons arriving from the other direction have a higher frequency of collisions and a reduced mean free path, which results in a decrease of electrical conductivity and, correspondingly, in an increase of energy dissipation and heat generation in the surface layer. Obviously, the closer the observation point $\boldsymbol{x}$ is to the surface the more severe are the required modifications, which implies that the relationship between the current and the electric field in the boundary layer can no longer be reduced to a simple proportionality with an $\boldsymbol{x}$-independent coefficient. Moreover, in the boundary layer the current $\boldsymbol{J}(\boldsymbol{x}, t)$ is not even necessarily parallel to the electric field $\boldsymbol{E}(\boldsymbol{x}, t)$.

## Appendix 3: The dielectric function in a metal

The macroscopic Maxwell equations (A1.9)–(A1.11) are not complete even when the relationship between the current $\boldsymbol{J}$ and the electric field $\boldsymbol{E}$ is known. To use these equations it is also necessary to establish connections between the induced polarization and magnetization fields $\boldsymbol{P}$ and $\boldsymbol{M}$, and the primary electric and magnetic fields $\boldsymbol{E}$ and $\boldsymbol{B}$. However, since our interest is restricted to good conductors like Au or Ag which have negligible magnetization [15, 34], for our purposes it suffices to assume that $\boldsymbol{M} = 0$, so that only the relationship between $\boldsymbol{P}$ and $\boldsymbol{E}$ needs to be established.

For sufficiently weak $\boldsymbol{E}$ it is natural to assume that the induced polarization $\boldsymbol{P}(x, t)$ depends linearly on the values of $\boldsymbol{E}(\xi, \tau)$ at all points $\xi$ and all times $\tau$ from the light cone $|x - \xi| < c(t - \tau)$. Since we are interested only in small domains where relativistic effects can be ignored, we may assume that the connection between $\boldsymbol{P}$ and $\boldsymbol{E}$ is described by the integral expression

$$\boldsymbol{P}(\boldsymbol{x}, t) = \epsilon_0 \int_{\tau < t} \iiint_G K(\boldsymbol{x}, \boldsymbol{\xi}, t - \tau) \boldsymbol{E}(\boldsymbol{\xi}, \tau) \mathrm{d}\boldsymbol{\xi} \mathrm{d}\tau, \qquad (A3.28)$$

where the kernel $K(\boldsymbol{x}, \boldsymbol{\xi}, t)$ should be defined either by taking into account the contributions of all elementary charges, or by phenomenological considerations based on some insightful models.

To discuss the structure of the kernels $K(x, \xi, t)$ it is convenient to assume that the time dependence of all fields is expressed by the factor $\mathrm{e}^{\mathrm{i}\omega t}$, that will be suppressed hereafter. Then, the Maxwell equations and constitutive relationships reduce to the form

$$\boldsymbol{\nabla} \cdot \boldsymbol{B} = 0, \qquad\qquad \boldsymbol{\nabla} \times \boldsymbol{E} = -\mathrm{i}\omega\boldsymbol{B}, \qquad\qquad (A3.29)$$

$$\boldsymbol{\nabla} \cdot \boldsymbol{D} = \rho, \qquad\qquad \boldsymbol{\nabla} \times \boldsymbol{H} = \mathrm{i}\omega\boldsymbol{D} + \boldsymbol{J}, \qquad\qquad (A3.30)$$

and

$$\boldsymbol{P}(\boldsymbol{x}) = \epsilon_0 \iiint_G \widehat{K}(\boldsymbol{x}, \boldsymbol{\xi}; \omega)\boldsymbol{E}(\xi)\mathrm{d}\boldsymbol{\xi}, \qquad\qquad (A3.31)$$

where the kernel is introduced by the one-sided Fourier integral

$$\widehat{K}(\boldsymbol{x}, \boldsymbol{\xi}; \omega) = \int_0^\infty K(\boldsymbol{x}, \boldsymbol{\xi}, t)\mathrm{e}^{-\mathrm{i}\omega t}\mathrm{d}t \qquad\qquad (A3.32)$$

which guarantees that it is an analytic function in the half-plane $\mathrm{Im}(\omega) \leq 0$.

Although the polarization $\boldsymbol{P}(\boldsymbol{x})$ at any specific point $\boldsymbol{x}$ is influenced by the electric field everywhere, only the field $\boldsymbol{E}(\boldsymbol{\xi})$ in a small domain $V_x$ around $\boldsymbol{x}$ makes significant contributions. However, the size of the domain of influence $V_x$ highly depends on the atomic structure of the material.

Consider again the free-electron model of metals used in the previous section for the estimates of the electric conductivity. In this model, positively charged ions are homogeneously distributed inside the body, and conduction electrons perform random motions governed by the equations (A2.14)–(A2.16) between random collisions which follow each other with the average frequency $\gamma$. Then, assuming, for simplicity, that the electric field has the structure (A2.17), we find from (A2.19) that the average displacement of the electron from its equilibrium position is described by the expression

$$\langle \Delta\boldsymbol{x}(t) \rangle = \frac{-\mathrm{i}q\boldsymbol{E}(\boldsymbol{x}, t)}{m_*\omega(\gamma + \mathrm{i}\omega)}. \qquad\qquad (A3.33)$$

Therefore, $\boldsymbol{p} = q\langle \Delta\boldsymbol{x}(t) \rangle$ is the dipole moment created by one electron, and counting contributions of all electrons we find that the polarization caused by the electric field $\boldsymbol{E}\mathrm{e}^{\mathrm{i}\omega t}$ has the value

$$\boldsymbol{P}(\omega) = \frac{-\mathrm{i}q^2 N\boldsymbol{E}(\boldsymbol{x}, t)}{m_*\omega(\gamma + \mathrm{i}\omega)} \equiv \frac{\sigma(\omega)}{\mathrm{i}\omega}\boldsymbol{E}(\boldsymbol{x}, t), \qquad\qquad (A3.34)$$

where $N$ is the number density of electrons. Then, combining (A3.34) with (A1.11) we get

$$\boldsymbol{D}(\boldsymbol{x}) = \epsilon_0\epsilon_r(\omega)\boldsymbol{E}(\boldsymbol{x}), \qquad\qquad (A3.35)$$

with the relative dielectric function

$$\epsilon_r(\omega) = 1 + \frac{\sigma(\omega)}{\mathrm{i}\omega\epsilon_0}. \qquad\qquad (A3.36)$$

Since the dielectric function of a metal is represented in terms of the electric conductivity $\sigma(\omega)$, it is obvious that the domain of applicability of the formulas (A3.35), (A3.36) can not be broader than the domain of applicability of (A2.23), (A2.24). Therefore, the proportionality relation

(A3.35) between the fields $\boldsymbol{D}$ and $\boldsymbol{E}$ with the $\boldsymbol{x}$-independent coefficient $\epsilon(\omega)$ from (A3.36) may not be valid in a boundary layer determined by the frequencies $\omega$ and $\gamma$ of field oscillations and electron collisions, respectively. In particular, in conductors like Au at room temperature in the optical band $\omega \sim 10^{15}$rad/s the formulas (A3.35), (A3.36) fail within a few nanometers from the metal surface.

Finally, for further purposes it is convenient and instructive to rearrange the expressions (A2.25) and (A3.36) to alternative forms. Thus, separating the real and imaginary parts, we can represent the complex-valued $\sigma$ and $\epsilon_r$ as

$$\sigma(\omega) = \sigma_1(\omega) + \mathrm{i}\sigma_2(\omega), \qquad \epsilon_r(\omega) = \epsilon_1(\omega) + \mathrm{i}\epsilon_2(\omega), \tag{A3.37}$$

with the real and imaginary parts defined either by the formulas

$$\sigma_1(\omega) = \frac{\sigma_0\gamma^2}{\omega^2 + \gamma^2}, \qquad\qquad \sigma_2(\omega) = \frac{-\sigma_0\gamma\omega}{\omega^2 + \gamma^2}, \tag{A3.38}$$

$$\epsilon_1(\omega) = 1 - \frac{\sigma_0\gamma}{\epsilon_0(\omega^2 + \gamma^2)}, \qquad\qquad \epsilon_2(\omega) = \frac{-\sigma_0\gamma^2}{\epsilon_0\omega(\omega^2 + \gamma^2)}, \tag{A3.39}$$

or by the formulas

$$\sigma_1(\omega) = \frac{\epsilon_0\gamma\omega_p^2}{\omega^2 + \gamma^2}, \qquad\qquad \sigma_2(\omega) = \frac{-\epsilon_0\gamma\omega\omega_p^2}{\omega^2 + \gamma^2}, \tag{A3.40}$$

$$\epsilon_1(\omega) = 1 - \frac{\omega_p^2}{\omega^2 + \gamma^2}, \qquad\qquad \epsilon_2(\omega) = \frac{-\gamma\omega_p^2}{\omega(\omega^2 + \gamma^2)}, \tag{A3.41}$$

where

$$\omega_p = \sqrt{\frac{q_e^2 N}{m\epsilon_0}} \tag{A3.42}$$

is the plasma frequency whose typical values for good conductors such as Au, Ag, or Cu at room temperature are of the order $\omega_p \sim 10^{16}$rad/s, [11, 15, 22, 35].

**Appendix 4: Electromagnetic fields in metals**

To understand the penetration of light into a metal it is instructive to consider a case when a metal occupying the half-space $x > 0$ is illuminated by a monochromatic electromagnetic wave arriving along the $x$-axis and described by the Maxwell equations (A3.29), (A3.30) supplemented by the constitutive relations $\boldsymbol{D} = \epsilon_0\epsilon_r\boldsymbol{E}$, $\boldsymbol{J} = \sigma\boldsymbol{E}$ and $\boldsymbol{H} = \epsilon_0 c^2\boldsymbol{B}$ where $\epsilon_0$ and $c$ are constants, while $\epsilon_r$ and $\sigma$ may depend on the frequency $\omega$ but do not depend on the spatial variables.

Let the metal be neutral, which means that $\rho = 0$. Then, we find from (A3.29), (A3.30) that $\boldsymbol{\nabla}\cdot\boldsymbol{E} = \boldsymbol{\nabla}\cdot\boldsymbol{H} = 0$, and using the identity $\boldsymbol{\nabla}\times\boldsymbol{\nabla}\times\boldsymbol{f} = \boldsymbol{\nabla}(\boldsymbol{\nabla}\cdot\boldsymbol{f}) - \boldsymbol{\nabla}^2\boldsymbol{f}$, find that

$$\boldsymbol{\nabla}\times\boldsymbol{\nabla}\times\boldsymbol{E} = -\boldsymbol{\nabla}^2\boldsymbol{E}, \qquad \boldsymbol{\nabla}\times\boldsymbol{\nabla}\times\boldsymbol{H} = -\boldsymbol{\nabla}^2\boldsymbol{H}, \tag{A4.43}$$

and combing these expressions with the above mentioned constitutive relations makes it possible to reduce the second equations from (A3.29) and (A3.29) to the forms

$$-\nabla^2 \boldsymbol{E} = -\mathrm{i}\omega \boldsymbol{\nabla} \times \boldsymbol{B} = -\frac{\mathrm{i}\omega}{\epsilon_0 c^2}\big(\mathrm{i}\omega \boldsymbol{D} + \boldsymbol{J}\big) = -\frac{\mathrm{i}\omega}{\epsilon_0 c^2}\big(\mathrm{i}\omega \epsilon_0 \epsilon_r + \sigma\big)\boldsymbol{E}, \tag{A4.44}$$

and

$$-\nabla^2 \boldsymbol{H} = \boldsymbol{\nabla} \times \big(\mathrm{i}\omega \boldsymbol{D} + \boldsymbol{J}\big) = \big(\mathrm{i}\omega \epsilon_0 \epsilon_r + \sigma\big)\boldsymbol{\nabla} \times \boldsymbol{E} = -\frac{\mathrm{i}\omega}{\epsilon_0 c^2}\big(\mathrm{i}\omega \epsilon_0 \epsilon_r + \sigma\big)\boldsymbol{H}. \tag{A4.45}$$

As a result we get the Helmholtz equations

$$\nabla^2 \boldsymbol{E} + k^2 \boldsymbol{E} = 0, \qquad \nabla^2 \boldsymbol{H} + k^2 \boldsymbol{H} = 0 \tag{A4.46}$$

with the wave number

$$k = k(\omega) = \sqrt{\frac{\epsilon_0 \epsilon_r(\omega)\omega^2 - \mathrm{i}\sigma(\omega)\omega}{\epsilon_0 c^2}}. \tag{A4.47}$$

Since the fields $\boldsymbol{E}$ and $\boldsymbol{B}$ are orthogonal to the direction of propagation and to each other, it is possible to assume that the $\boldsymbol{E}$ is parallel to the $y$-axis and $\boldsymbol{B}$ is parallel to the $z$-axis. Then

$$\boldsymbol{E} = E\boldsymbol{e}_y, \qquad \boldsymbol{H} = H\boldsymbol{e}_z \tag{A4.48}$$

where $E$ and $H$ are the scalar fields

$$E = E_0(y, z)\, e^{-\mathrm{i}kx}, \qquad H = H_0(y, z)\, \mathrm{e}^{-\mathrm{i}kx}. \tag{A4.49}$$

Since the $k$ defined by (A4.47) is a complex number, the fields (A4.49) exponentially decay inside the material which implies that the electromagnetic radiation does not penetrate inside the metal beyond the distance determined by the imaginary part of the wave number.

To estimate the depth of penetration of the fields (A4.49) into the metal, we recall (A2.25) and (A3.36) and reduce (A4.47) to

$$k = k_1 + \mathrm{i}k_2 = \sqrt{\frac{\epsilon_0 \omega^2 - 2\mathrm{i}\sigma\omega}{\epsilon_0 c^2}} = \sqrt{\frac{(\epsilon_0 \omega^2 + 2\sigma_2\omega) - 2\mathrm{i}\omega\sigma_1}{\epsilon_0 c^2}}, \tag{A4.50}$$

where $\sigma_1$ and $\sigma_2$ have real values defined by (A3.38). Then, we readily get the explicit formulas

$$k_1^2 = \frac{1}{c\sqrt{\epsilon_0}}\left(\sqrt{(\epsilon_0\omega^2 + 2\sigma_2\omega)^2 + 4\omega^2\sigma_1^2} + \epsilon_0\omega^2 + 2\sigma_2\omega^2\right) > 0, \tag{A4.51}$$

$$k_2^2 = \frac{1}{c\sqrt{\epsilon_0}}\left(\sqrt{(\epsilon_0\omega^2 + 2\sigma_2\omega)^2 + 4\omega^2\sigma_1^2} - \epsilon_0\omega^2 - 2\sigma_2\omega^2\right) > 0. \tag{A4.52}$$

This result shows that in the domain $x > h$, with $h$ from (A2.27), where "local" constitutive relations (A3.35), (A3.36) and Ohm's law (A2.24), (A2.25) hold, such fields in (A4.49) decay proportionally to $e^{-|k_2|(x-h)}$. Correspondingly, the so called skin depth

$$\delta(\omega) = \frac{1}{|\operatorname{Im} k_2(\omega)|} \tag{A4.53}$$

17

characterizes the penetration of the electromagnetic radiation into the metal. It is well known that in the low frequency range $\omega \ll \gamma$ the skin depth depends on the frequency as $\delta \approx \sqrt{2c^2/\epsilon_0 \sigma_0 \omega}$ but at high frequencies $\omega \gg \gamma$ it stabilizes at the level $\delta \sim c/\omega_p \approx 20$nm, where $\omega_p$ is the plasma frequency from (A3.42) and the numerical estimate corresponds to Au at room temperature.

As discussed in the end of Section 2, the conditions that lead to the expression (A4.52) are not valid in the boundary layer of depth $h \sim \min\{l_*, l_\circ\}$ from (A2.27), where $l_*$ is the mean free path of conduction electrons and $l_\circ$ is the mean path that these electrons travel in one cycle of the field oscillation. At optical frequencies in good conductors like Au and Ag, at room temperature $l_\circ \sim 3$nm and $l_* \sim 30$nm, so that $h \sim 3$nm, while the skin depth is of order of $\delta \sim 20$nm.

All of the above implies that in order to describe the penetration of light into good conducting metals it is necessary to consider three different zones as illustrated in Fig. 1.

First, there is a narrow, a few nanometers thick, surface layer $0 < x < h$ in which neither Ohm's law (A2.24), (A2.25) nor the constitutive relations (A3.35), (A3.36) are valid. In this layer the fields cannot be described by macroscopic Maxwell equations and have a complicated structure heavily dependent on the surface of the metal. Since the thickness of this layer is comparable with the roughness of the surfaces, the processes in this layer may be considered as surface phenomena.

Next, there is a skin layer $h < x < h + \delta$ of thickness $\delta \sim 20$nm, where the electromagnetic field is described by the macroscopic Maxwell equations with the local constitutive equations and Ohm's law, which imply that the fields exponentially decay as $\mathrm{e}^{-(x-h)|\operatorname{Im}(k_2)|}$, where $k_2$ is defined by (A4.52) and $(x - h)$ is the depth measured from the interior side of the surface layer.

Finally, the interior of any metal is inaccessible for light. In particular, optical fields penetrate good conductors at room temperature only within the layer of the thickness $h + \delta \sim 25$nm, which can be ignored in many cases, but not in modern nano-scale devices.